Journal of Environmental Management 349 (2024) 119568

Contents lists available at ScienceDirect

Journal of Environmental Management

journal homepage: www.elsevier.com/locate/jenvman

Research article

Photo driven homogeneous advanced oxidation coupled to adsorption process for an effective arsenic removal from drinking water

Anna Melnikova [a,1], Antonio Faggiano [b,1], Marco Visconti [b], Raffaele Cucciniello [b], Patrizia Iannece [b], Natalia Kostryukova [a], Antonio Proto [b], Antonino Fiorentino [b,*], Luigi Rizzo [c]

[a] Department of Environmental Health & Safety, Ufa University of Science and Technology, Zaki Validi 32, 450076, Ufa, Republic of Bashkortostan, Russian Federation
[b] Department of Chemistry and Biology "A. Zambelli", University of Salerno, Via Giovanni Paolo II 132, 84084, Fisciano, SA, Italy
[c] Water Science and Technology (WaSTe) Group, Department of Civil Engineering, University of Salerno, Via Giovanni Paolo II 132, 84084, Fisciano, SA, Italy

ARTICLE INFO

Handling Editor: Prof Raf Dewil

Keywords:
Advanced oxidation processes
Drinking water
Heavy metals
UVC/NaOCl
UVC/H_2O_2

ABSTRACT

The presence of arsenic (As) in drinking water is a major concern for human health. As(III) is the most toxic water-soluble form and it is hard to remove by separation methods, including adsorption, while As(V) is less toxic and easily removable by adsorption. In this work homogenous photo driven advanced oxidation processes (HP-AOPs), namely UVC/H_2O_2 and UVC/NaOCl, have been investigated in the oxidation of As(III) (initial concentration of 0.1 mg/L) to As(V) and commercial available adsorbents (γ-Al_2O_3, Bayoxide E33, MgAl-LDHs and ZnAl-LDHs) were tested for subsequent As(V) removal. UVC/H_2O_2 (99% of As removal, 19 mg/L of H_2O_2, 2 min of treatment time) and UVC/NaOCl (99% of As removal, 5.1 mg/L of NaOCl, 2 min of treatment time) were found to be more effective than H_2O_2 (2% of As removal in the same condition of UVC/H_2O_2) and NaOCl (6% of As removal in the same condition of UVC/NaOCl), respectively and the optimum operation conditions were identified by response surface methodology (RSM) in distilled water and subsequently confirmed in real drinking water (with differences of less than 1%). UVC/NaOCl was the most suitable process being a good compromise among oxidation efficiency, oxidant dose and treatment time. The best results in terms of subsequent removal of As(V) by adsorption were obtained using ZnAl-LDH (88% in both distilled and drinking water). Accordingly, UVC/NaOCl advanced oxidation coupled to ZnAl-LDH adsorption is the best combination for an effective removal of arsenic from drinking water.

1. Introduction

Arsenic (As) is a common element that can be found in atmosphere, soil, rocks, water and living organisms. Its presence in nature is caused by atmospheric reactions, volcanic activity, as well as several anthropogenic activities, such as mining and fuel combustion (Zhang et al., 2022). The presence of As in water, when it is used as drinking water, for aquaculture or agricultural irrigation, is a major problem. It was estimated that about 150 million people drink water that exceeds the maximum levels of contamination for As in drinking water (10 μg/L) (Liu and Qu, 2021). Consumption of water contaminated with As can cause serious problems for people's health, such as various forms of cancer, diseases of the cardiovascular, nervous and endocrine systems and diabetes (Masindi and Gitari, 2016). Arsenic can accumulate in human body, penetrating through hair, nails and skin, making hair, urine and nails ideal biomarkers (Goswami et al., 2020). In natural waters, As is found in organic (monomethyl-As) and non-organic forms (arsenite As(III) and arsenate As(V)). Depending on the chemical nature of As, its characteristics change, such as adsorption properties, mobility and toxicity (Singh Patel et al., 2023). According to the literature, As(III) is the most toxic water-soluble substance, while As(V) is less toxic. High levels of As in groundwater have been found in many countries such as Chile, Argentina, Hungary and India (Alam et al., 2023; Bundschuh et al., 2021). Italy is another country with a high concentration of As in groundwater, especially in Lombardy, Vento, Emilia-Romagna, Tuscany and Lazio regions (Ghezzi et al., 2023; Sorlini and Collivignarelli, 2011). In 1933, the World Health Organization (WHO) reduced the recommended value of As in drinking water from 50 μg/L to 10 μg/L due to increasing evidence of its toxic effects on humans (World Health Organizaion, 2022). In Italy, the recommended concentration of As in water is also 10 μg/L, this limit was adopted by Legislative Decree

* Corresponding author.
E-mail address: afiorentino@unisa.it (A. Fiorentino).
[1] These authors contributed equally to the manuscript.

https://doi.org/10.1016/j.jenvman.2023.119568
Received 26 September 2023; Received in revised form 31 October 2023; Accepted 4 November 2023
Available online 15 November 2023

List of abbreviation

AOPs	Advanced oxidation processes
As	Arsenic
RSM	response surface methodology
WHO	World Health Organization
LDH	layered double hydroxides

18/2023, following the adoption of European Directive EU 2020/2184 (European Parliament and Council, 2020).

Methods for removing As from water can be divided into four main groups: ion exchange, membrane-based filtration, precipitation, and adsorption. Typically, adsorption process is more effective in the removal of As(V), therefore a pre-oxidation of As(III) to As(V) will improve subsequent adsorption process efficiency (Hao et al., 2018; Jadhav et al., 2018). Among the most investigated adsorbents, Fe–Mn composite oxides (Liu et al., 2022), γ-Al_2O_3 (Iervolino et al., 2016), iron-based adsorbents (Hao et al., 2018) for As removal, layered-double hydroxides (LDHs) have gained an increasing interest (Lee et al., 2018). LDH is a class of multi-metal lamellar materials represented by the formula $[M^{II}_{1-x}M^{III}_{x}(OH)_2]^{x+}(A^{y-})_{x/y}\bullet zH_2O$, with divalent ($M^{II}$) and trivalent ($M^{III}$) metallic cations, and charge compensating anions (A^{y-}) that can be readily replaced in the interlayer regions (Fierro et al., 2023). Based on the ion exchange of the interlayer anions this class of materials can effectively acts as valuable candidate for As(V) removal. Previous works on As(V) removal from aqueous matrices have investigated initial As(V) concentration in the range 1–100 mg/L (Gupta et al., 2021). However, it is worth noting that As(V) occurs at significantly lower concentrations (about 100 μg/L) in groundwater in different geographical areas (Shaji et al., 2021; Sorlini and Collivignarelli, 2011).

Oxidation of As(III) to As(V) by different oxidants, such as ozone, chlorine, potassium permanganate, hydrogen peroxide, etc. was investigated (Amiri et al., 2022; Dodd et al., 2006; Lee et al., 2011). However, conventional oxidation processes are not so effective or result in the formation of toxic and regulated oxidation by products, such as trihalomethanes (chlorination by-products), chlorite and chlorate (chlorine dioxide by-products) and bromate (ozonation by-products) (Srivastav et al., 2020) Therefore, alternative processes such as advanced oxidation processes (AOPs) have been investigated as possible alternative option (Abenza et al., 2023; Faggiano et al., 2023; Zaw and Emett, 2002). In particular, heterogeneous photo driven AOPs have been successfully investigated in the oxidation of As(III) to As(V) (Chianese et al., 2023; Liu et al., 2022; Vaiano et al., 2014, 2018), but they still suffer of scale-up limitations which make them not yet competitive with consolidated technologies (Fiorentino et al., 2017; Iervolino et al., 2019). On the opposite, homogenous photo driven AOPs (HP-AOPs), such as UVC/H_2O_2 and UVC/NaOCl, have been successfully investigated in different applications to water and wastewater treatment and are either already applied at full scale in wastewater treatment for potable reuse (UVC/H_2O_2) or easy to scale-up (Rizzo, 2022).

In this work HP-AOPs, namely UVC/H_2O_2 and UVC/NaOCl, were investigated in the oxidation of As(III) to As(V) and subsequently coupled to adsorption process for the removal of As(V) for drinking water, for the first time. Tests with NaOCl and H_2O_2 were also carried out and the operating conditions of the HP-AOPs were optimized through the support of a two-level factorial design coupled with response surface methodology (SM), first in distilled water and subsequently confirmed in real drinking water. The operating conditions were optimized in terms of oxidant concentration, treatment time, oxidant type, with and without UVC light (target responses). Finally, commercial and easy-to-handle adsorbents, namely γ-Al_2O_3, Bayoxide E33, MgAl-LDHs and ZnAl-LDHs, were tested for As (V) removal in both distilled and real drinking water after the oxidation step.

2. Materials and methods

2.1. Reagents

Sodium (meta) arsenite ($NaAsO_2$), hydrogen peroxide (H_2O_2), sodium hypochloride (NaClO) with 10% of active Cl_2, ascorbic acid ($C_6H_8O_6$), potassium iodide (KI), hydrochloric acid (HCl), nitric acid (HNO_3), sodium hydroxide (NaOH), sodium thiosulfate ($Na_2S_2O_3$), titanium(IV) oxysulfate ($TiOSO_4$) and sodium borohydride ($NaBH_4$) were purchased from Sigma-Aldrich and used as bought without modification. γ-Al_2O_3 (Puralox SCCa-5/200) was provided by Sasol. Bayoxide E33, granular form, was purchased by Lanxess (Koeln, Germany). MgAl and ZnAl layered double hydroxides with chloride and nitrate ions as interlayer anions and MgAl mixed oxides were purchased by Prolabin and Tefarm S.r.l. (Perugia, Italy).

2.2. Synthetic aqueous solutions and real drinking water

Water treatment tests were carried out first in distilled water and subsequently in real drinking water purposely spiked with $NaAsO_2$ (0.1 mg/L of As(III)). Drinking water samples were collected from a tap of Fisciano campus of the University of Salerno (Table 1).

2.3. Experimental set-up

Oxidation experiments with H_2O_2 and NaOCl were carried out with the aim of UVC radiation and in dark conditions (to evaluate the effect of the radiation on the oxidation process). Oxidation time in the range 15–120 min and oxidant concentration in the range 1–15 mg/L were chosen as input data for the software. In UVC driven advanced oxidation experiments, UVC radiation was provided by a 16 W lamp with an emission peak at 254 nm (Sankyo Denky GT10T5L) positioned vertically in a 1 L (5 cm diameter) cylinder filled with 500 mL of aqueous sample. The oxidant was added to the sample and then the UVC lamp was switched on (time zero). The light intensity of the lamp (4.7 mW s/cm2) was measured by a HR2000 (Ocean Optics, Florida, USA) radiometer. Experiments in dark conditions with H_2O_2 and NaOCl were also carried out using treatment time till to 120 min and oxidant concentration in the range 1–15 mg/L as input data for the software. The dark oxidation experiments were carried out in the same reactor, completely covered by aluminium paper, under continuous stirring, with UVC lamp switched off. The temperature was kept constant at 25 ± 1 °C with a thermostatic probe.

2.4. Analytical measurements

Temperature, pH and electrical conductivity were measured by pH-EC-TDS Temperature Portable Meter Hanna 9812–5. H_2O_2 concentration in water was determined spectrophometrically through a $TiOSO_4$ based method, as described in a previous work (Fiorentino et al., 2015). Residual free chlorine concentration was measured by Hach Pocket

Table 1
Characteristics of real drinking water.

Parameter	Concentration[a]
pH	6,9
Free carbon dioxide at the source	15
Ca^{2+}	86,2
Mg^{2+}	12
Na^{+}	3,4
Cl^{-}	5,3
K^{+}	1
NO_3^{-}	3,1
F^{-}	0,1

[a] All the concentration are expressed in mg/L except for pH, which is unitless.

Colorimeter™, through DPD method. Total As concentration was measured by ICP-OES through pre-reduction of As(V) to As(III) with 1.0 % KI (in 0.2 % ascorbic acid) and 3.0 mol/L HCl (Welna et al., 2019). An aliquot of 7.5 mL of each sample solution was transferred to a 15 mL volumetric flask; then 1.5 mL of 10 % KI in 2.0 % ascorbic acid and 3.75 mL of concentrated HCl were added and left to react for about 30 min. Simultaneously, 20 mL of the treated sample were passed through LC-SAX cartridge (Supelclean™ LC-SAX SPE Tube from Supelco) to retain As(V), and As(III) concentration was measured by ICP-OES. This procedure allowed to calculate As(V) concentration as difference between total As and As(III).

2.5. Experimental design

In this study, RSM was used for the experimental design of the oxidation processes. The dosage of H_2O_2 and NaOCl (X1) and treatment time (X2) were selected as numerical factors, while presence/absence of radiation (X3) and the type of oxidant (X4) were selected as categorical factors. The experimental design involved 31 runs, based on a two-level central composite factorial design. The levels (i.e., the values chosen to vary the independent variables to study how they influence the output response and obtain valuable information for process optimization) for each variable are provided in Table 2.

The response was estimated through a second-order polynomial equation according to Eq. (1):

$$Y = b_0 + \sum_{i=1}^{n} b_i X_i + \sum_{i=1}^{n} b_{ii} X_i^2 + \sum_{i=1}^{n} b_{ij} X_i X_j + \varepsilon \quad (1)$$

where Y is the response of As(III) oxidation, b_0 is a constant, b_i correspond to the linear coefficient of X_i, b_{ii} is the second order effect on regression coefficients, b_{ij} is the interaction coefficient and ε is the statistical error.

After the calculation of the optimal process for As(III) oxidation, three replicates of this process were made and the kinetics were calculated.

For the optimization of the process, the following conditions were used:

- Oxidant dose in the range 1–30 mg/L;
- Minimization of treatment time;
- Radiation: UVC or dark.
- Oxidant type: H_2O_2 or NaOCl.

The following goals were selected for the responses:

- As(III) oxidation >95.0% to reach a final concentration below World Health Organization limit (World Health Organizaion, 2022) for drinking water (0.01 mg/L).

Table 2
Ranges and levels of designed factors.

Variable	Code	Levels				
		L1	L2	L3	L4	L5
Oxidant concentration (mg/L)	X1	1	5	10	15	30
Treatment time (min.)	X2	5	10	15	60	120
Radiation	X4	UVC	Dark	–	–	–
Oxidant type	X3	H_2O_2	NaOCl	–	–	–

RSM design for the three experimental variables in coded units and the corresponding natural values are listed in Tables SM1 and SM2 of the supplementary material file. The response taken in consideration for RSM analysis was the As (III) percentage removal.

2.6. Adsorption experiments

Adsorption experiments for the removal of As(V), produced during the photocatalytic reaction, were carried out in a 250 mL beaker in the absence of UV radiation using 50 and 100 mL of solution containing a known concentration of As(V) (100 μg/L) and stirred for 1 and 5 min with 0.02 g of the adsorbing material. Then the adsorbent was filtered-off and the As(V) concentration in solution was determined by ICP-OES as described in Section 2.4. The best two adsorbents were finally compared for tests in real drinking water. In detail, 100 mL of drinking water containing As(V) (100 μg/L) was stirred for 1, 5, 15 and 30 min in the presence of 0.02 g of adsorbing material in a 250 mL beaker. All the experiments were carried out at room temperature. Results are expressed as percentage As(V) removal.

3. Results and discussion

3.1. Experimental and statistical model

Based on the results from the quadratic model, the empirical relationship between the response and the independent variables is:

$$\text{As(III)oxidation}[\%] = 76.17 + 1.5X_1 + 2.4X_2 - 21.3X_3 + 20.3X_4 - 1.9X_1X_2 + 1.2X_1X_3 + 3.7X_1X_4 - 0.3X_2X_3 - 4.2X_2X_4 + + 20.7X_3X_4 - 6.6X_1^2 + 1.5X_2^2 \quad (2)$$

F-value of the model was 40.72 (p-value <0.05 and $R^2 = 0.99354$), indicating that the model is statistically significant. This means that the results obtained from the model are highly likely to be true, and the variables in the model have a significant relationship. P-values lower than 0.05 indicate that the model terms are significant as well. In this case X_2, X_3, X_4, X_1X_4, X_2X_4, X_3X_4, X_1^2 are significant parameters, a good correlation between the empirical model and the actual values being achieved.

3.2. NaOCl and UVC/NaOCl tests

The oxidation processes using NaOCl and UVC/NaOCl for As(III) oxidation were investigated. Specifically, the NaOCl process was compared with the UVC/NaOCl process to explore the possible advantages that the combination of chlorine with UVC radiation can offer. By using UVC radiation, the need for higher chlorine dosages can be reduced, potentially lowering the formation of harmful disinfection by-products. The optimal NaOCl concentrations for both processes were determined by RSM (Fig. 1).

The perturbation plot illustrates the impact of NaOCl initial concentration (Line A) and treatment time (Line B) on the model's response for NaOCl (Fig. 1a) and UVC/NaOCl (Fig. 1c) treatments. This plot allows to assess the model's sensitivity to changes in the input variables, with steeper slopes indicating higher sensitivity and flatter slopes indicating lower sensitivity. By analyzing this plot, it is possible to gain valuable insights into how variations in the input factors affect the model's output.

The 3D surface plots (Fig. 1b and d, for NaOCl and UVC/NaOCl, respectively)show the relationship between the same input variables from the perturbation plot and the response variable. In this representation, the two input variables are mapped on the X and Y axes, while the response variable is displayed on the Z-axis. By examining the response surface plots, it is possible to understand better the complex interactions between the input variables and their impact on the response. This plot is useful to identify regions of optimal response and provides a deeper understanding of the overall behaviour of the model in a three-dimensional space.

The perturbation plots show the response changes as each factor moves from the chosen reference point. The values −1, −0.5, 0, +0.5 and + 1 on the x-axis represent the lower, the lower intermediate, the middle, the upper intermediate and the upper levels of the factors

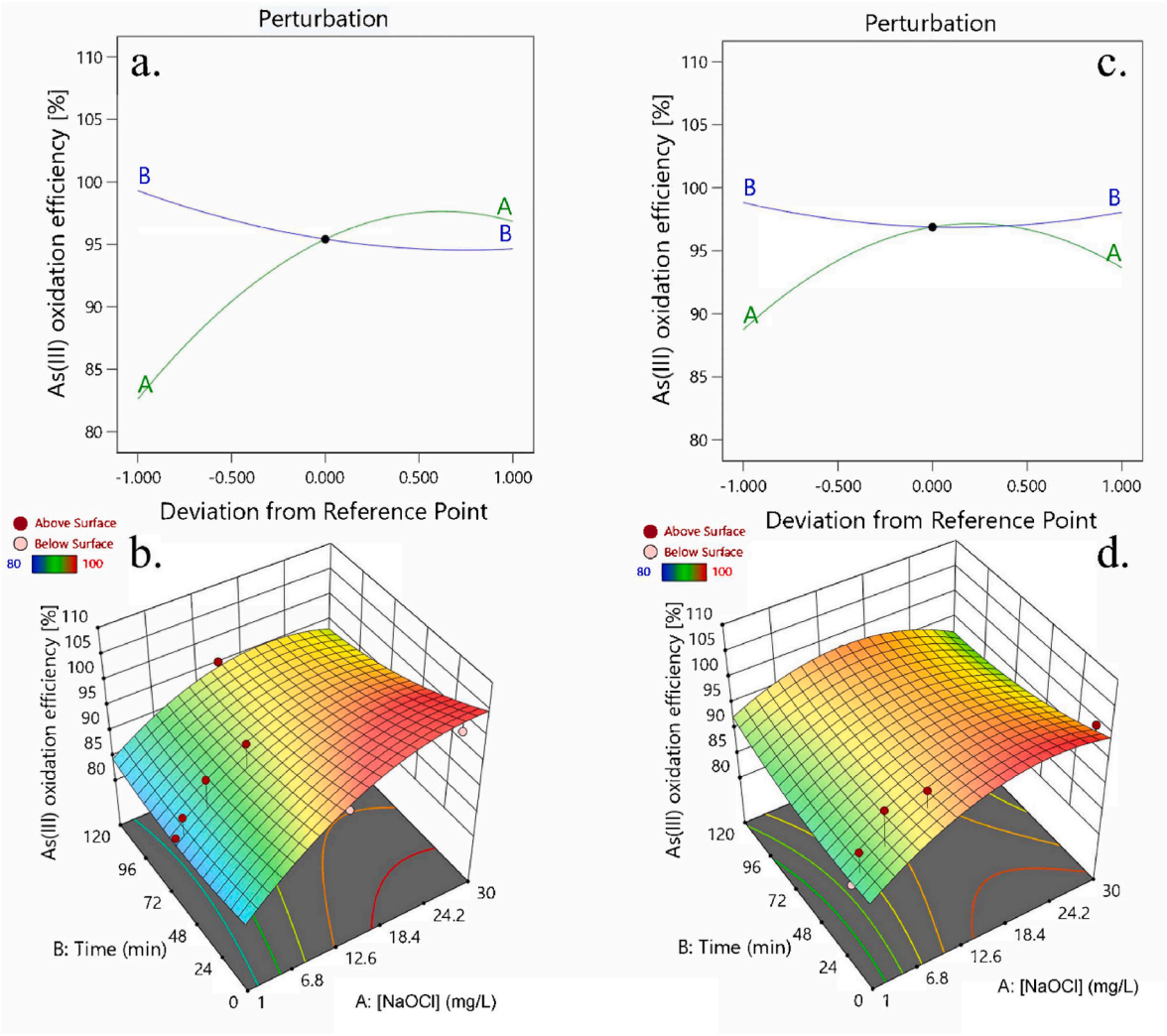

Fig. 1. Perturbation plots (a,c) and response surface plot (b,d) by NaOCl (a, b) and UVC/NaOCl (c,d) for As(III) oxidation. In the perturbation plot the line A and B correspond to NaOCl concentration and treatment time respectively.

investigated by the experimental design (this applies to all subsequent graphs), respectively. In all perturbation plots of this work the reference point was set at the midpoint (coded in the experimental design as 0). In the discussion of each perturbation plot, the positive effect means that the response increases with the enhancement of the factor level and the negative effect means that response decreases due to the increase of the factor level.

In the case of NaOCl processes (Fig. 1a and c), As(III) oxidation efficiency increased as the oxidant dose was increased. In dark condition, the oxidation efficiency increased from 78% with a minimum NaOCl concentration of 1 mg/L to 97% with a maximum NaOCl concentration of 30 mg/L. Likewise, the treatment time to reach the maximum oxidation efficiency decreased from 120 min with 1 mg/L of NaOCl to 15 min with 30 mg/L of NaOCl. As it can be seen from the perturbation plot, in the case of NaOCl the oxidant concentration has a positive effect on oxidation efficiency until the middle point, after which a plateau can be observed. The time, similarly to the oxidant effect, shows an almost constant trend. In UVC/NaOCl process (Fig. 1 c, d) oxidant concentration and treatment time show a trend similar to NaOCl process alone but, after the middle-point, the negative effect of oxidant concentration is higher. Coupling UVC radiation to chlorine increased oxidation efficiency compared to NaOCl alone (about 99% with NaOCl concentrations over 5 mg/L). In particular, an oxidation of 99% was reached with 5, 10 and 30 mg/L after 15, 13 and 10 min, respectively.

In a recent work the oxidation of As(III) was investigated by H_2O_2, O_3, and NaOCl (Amiri et al., 2022) using RSM. NaOCl was found to be the best oxidant reaching an oxidation efficiency of 99.5% of As(III) (initial concentration of 5 mg/L and final concentration of 0.025 mg/L) with about 9 mg/L of active Cl_2 in 4 min treatment. The results are also in agreement with another previous work, where oxidation of As (III) using various oxidants (namely, NaClO, $KMnO_4$, ClO_2, NH_2Cl) was investigated (Sorlini and Gialdini, 2010). In particular, the authors observed an As(III) oxidation efficiency of about 80% with NaOCl in dark condition, after 5 min of treatment dosing the oxidant at a higher initial concentration than the stoichiometric dose. The mechanism of As oxidation by NaOCl in dark conditions can be explained through the following equation (Sorlini and Gialdini, 2010):

$$H_3AsO_3 + Na^+ + ClO^- \rightarrow H_2AsO_4^- + Na^+ + Cl^- + H^+ \quad (3)$$

UVC/NaOCl process leads to the formation of highly reactive chlorine, hypochlorite and hydroxyl radicals according to the following equations (Eqs. (4)–(10)) (Lescano et al., 2012; Rizzo, 2022):

$$HOCl + h\nu \rightarrow HO^\bullet + Cl^\bullet \quad (4)$$

$$OCl^- + h\nu \rightarrow O^{\bullet -} + Cl^\bullet \quad (5)$$

$$O^{\bullet -} + H^+ \rightarrow HO^\bullet \quad (6)$$

$$HOCl + HO^\bullet \rightarrow + ClO^\bullet + H_2O \quad (7)$$

$$OCl^- + HO^\bullet \rightarrow + ClO^\bullet + OH^- \quad (8)$$

$$HOCl + Cl^\bullet \rightarrow ClO^\bullet + H^+ + Cl^- \quad (9)$$

$$OCl^- + Cl^\bullet \rightarrow ClO^\bullet + Cl^- \quad (10)$$

While the oxidation mechanism of As(III) by chlorine radicals remains a topic that lacks comprehensive understanding, such radicals are expected to make the oxidation reaction of As(III) to As(V) faster and different studies in the literature have consistently reported its occurrence (Amiri et al., 2022; Sorlini and Gialdini, 2010). This intriguing phenomenon underscores the importance of directing research efforts towards gaining deeper insights into this aspect. As such, further investigations are warranted to elucidate the intricacies of this chemical reaction, potentially shedding light on its implications in various environmental and health contexts.

3.3. H_2O_2 and UVC/H_2O_2 tests

To compare the potential increase in oxidation rate using UVC radiation, and to compare these two processes with those using NaOCl, oxidation of As(III) by UVC/H_2O_2 and H_2O_2 alone processes were investigated. The optimal H_2O_2 concentrations for both processes were determined by RSM (Fig. 2).

Even in this case, the photo-assisted oxidation was more effective than oxidation process alone. In the case of the dark process, H_2O_2 residual concentrations higher than 0.2 mg/L were detected for each test. UVC/H_2O_2 process, instead, allowed to reach high oxidation efficiencies (>98%) and very fast oxidant consumption resulted in a low residual (<0.2 mg/L) within a few minutes of treatment (about 2 min). H_2O_2 process (Fig. 2 a, b), showed a very poor As(III) oxidation efficiency even compared to NaOCl and UVC/NaOCl. In fact, the oxidation efficiency varied from a minimum of less than 1% (1 mg/L of H_2O_2 after 10 min treatment) to a maximum of 28% (15 mg/L H_2O_2 after 120 min treatment). The concentration of H_2O_2 resulted in a positive effect on oxidation efficiency up to the midpoint and subsequently a negative trend can be observed. In contrast to the NaOCl process, the treatment time shows a strongly positive effect and thus in this case oxidation efficiencies increase as treatment time increases. Instead, when the UVC radiation was coupled to H_2O_2 process, efficiency drastically increased, with a minimum of 88% oxidation with 30 mg/L of H_2O_2 after 10 min of treatment up to a maximum of 98% with 15 mg/L of H_2O_2 after 15 min. As in the case of the H_2O_2 process, the treatment time has a positive effect on removal efficiencies, while the concentration of the oxidising agent has a first slightly positive effect followed by a strongly negative effect after the midpoint. In fact, the highest efficiencies are obtained at highest treatment times (Fig. 2d), unlike of the UVC/NaOCl process in which very high efficiencies are achieved for all the experimental conditions (Fig. 1d).

The oxidation of As(III) through H_2O_2 can be described through the following reaction (Eq. (11)) (Amiri et al., 2022):

$$H_3AsO_3 + H_2O_2 \rightarrow H_2AsO_4^- + H_2O + H^+ \quad (11)$$

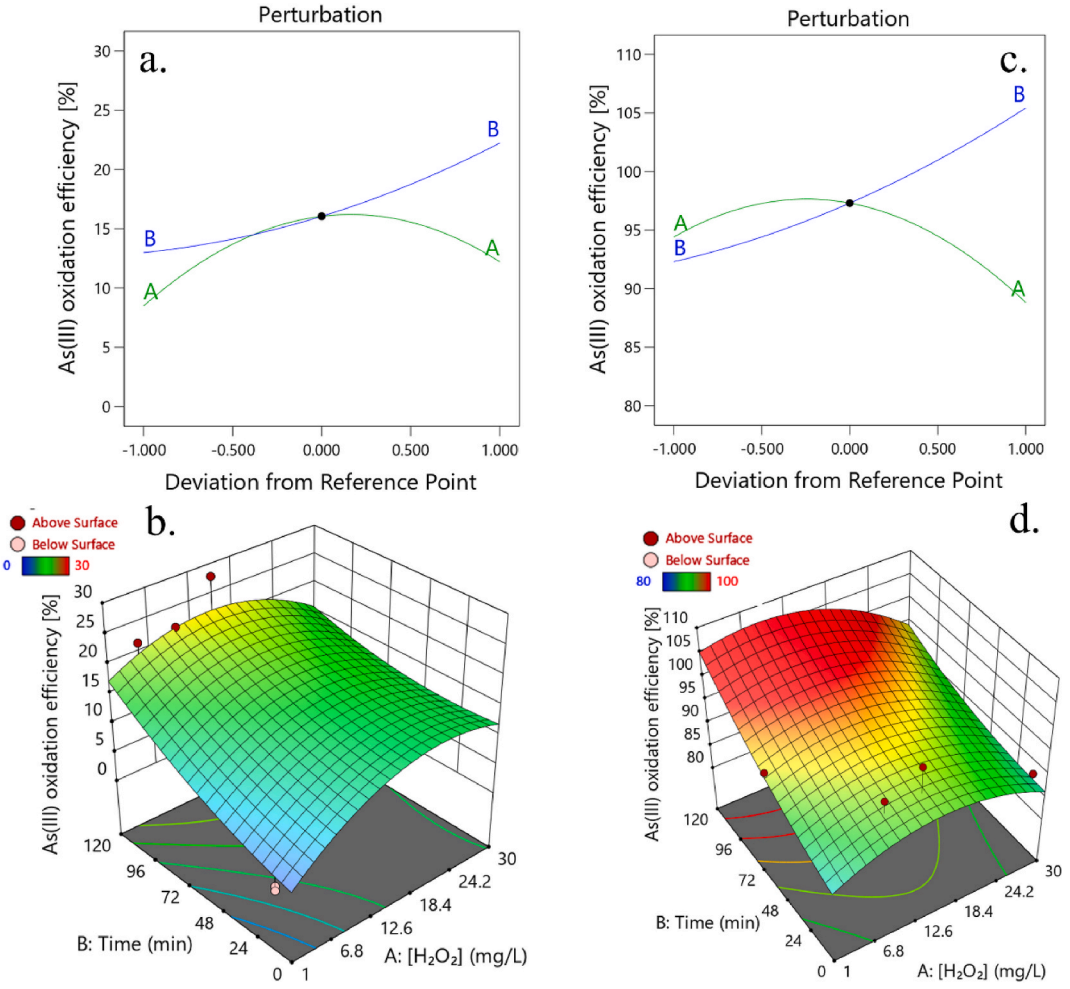

Fig. 2. Perturbation plots (a,c) and response surface plot (b,d) by H_2O_2 (a,b) and UVC/H_2O_2 (c,d) for As(III) oxidation. In the perturbation plot the line A and B correspond to H_2O_2 initial concentration and treatment time, respectively.

Previously, Sorlini et al. investigated the oxidation of As(III) (initial concentration of 0.1 mg/L) with 5 mg/L of H_2O_2 (Sorlini et al., 2010). In their work only the 5.8 % was reached for As(III) oxidation to As(V). The lower oxidation efficiency of As(III) obtained in their work is most likely due to the low dose of H_2O_2 used (5 mg/L) since, in the present work, RSM allowed to identify 30 mg/L as the optimal dose of H_2O_2 for the oxidation of As(III) (at the same initial concentration of As(III)). In fact, at low H_2O_2 concentration, the oxidation efficiency was comparable. In particular, at the H_2O_2 concentration of 5 mg/L tested in this work, the maximum oxidation efficiency was 21 %.

According to Lescano et al. (2012), the mechanisms for As oxidation by the UVC/H_2O_2 process are (Eq. (12) – Eq. (20)):

$$H_2O_2 + hv \rightarrow 2\ HO^{\bullet} \quad (12)$$

$$H_2O_2 + HO^{\bullet} \rightarrow HOO^{\bullet} + H_2O \quad (13)$$

$$HOO^{\bullet} + HO^{\bullet} \rightarrow O_2 + H_2O \quad (14)$$

$$2\ HO^{\bullet} \rightarrow H_2O_2 \quad (15)$$

$$H_3AsO_3 + HO^{\bullet} \rightarrow HAsO_3^{\bullet -} + H^+ + H_2O \quad (16)$$

$$H_3AsO_3 + HOO^{\bullet} \rightarrow HAsO_3^{\bullet -} + HOO^- + 2H^+ \quad (17)$$

$$HAsO_3^{\bullet -} + O_2 + H_2O \rightarrow H_2AsO_4^- + HOO^{\bullet} \quad (18)$$

$$H_3AsO_3 + H_2O_2 \rightarrow H_2AsO_4^- + H^+ + H_2O \quad (19)$$

$$H_3AsO_3 + O_2 + H_2O \rightarrow H_2AsO_4^- + H^+ + H_2O_2 \quad (20)$$

Lescano et al. (2012) also investigated the oxidation of As(III) (0.2 mg/L) by UVC/H_2O_2 process and they found that 15 mg/L of H_2O_2 was the best concentration for the oxidation process, obtaining about 99 % of As(III) oxidation in 10 min of treatment time, in agreement with our results.

As in the case of processes with NaOCl, an increase in oxidation efficiencies and a decrease in treatment time was observed with the addition of UVC radiation to H_2O_2. As in the previous case, this can be attributed to the formation of hydroxyl and hydroperoxyl radicals that allow the reaction rate to increase.

3.4. Kinetics of As(III) oxidation in real drinking water

According to RSM analysis, the optimum conditions to oxidise As(III) to As(V) in this work are summarized in Table 3.

The results show that a double dose of chlorine and a treatment time of 10 min are needed to obtain the same oxidation efficiency of As(III) compared to the photo-activated process (2 min). Therefore, the use of chlorine alone involves a higher risk of formation of chlorination by-products (in particular of trihalomethanes (THMs)) and a larger volume (for the higher hydraulic time retention) of the reactor. In fact, it is well known that the formation of THMs increases as chlorine dose and the contact time increase, and it is affected by the characteristics of the water in terms of total organic carbon (TOC), oxidant demand and bromine ion concentration (Sikder et al., 2023).

The kinetics for each optimized condition (Fig. 3a for UVC/NaOCl and NaOCl and Fig. 3b for UVC/H_2O_2 and H_2O_2) were performed to validate the RSM results as well as to evaluate the feasibility of the processes also with respect to the compliance of the residual oxidant concentration with standards for drinking water. For each process, kinetic order and constant were evaluated (Table 4).

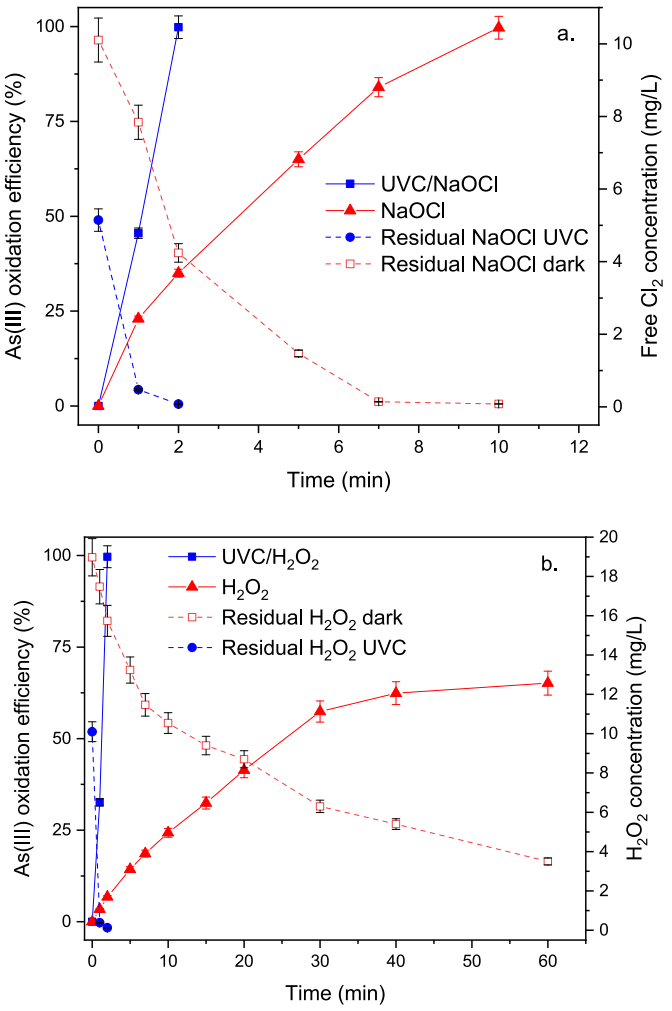

Fig. 3. UVC/NaOCl, NaOCl kinetics, chlorine consumption (a) and UVC/H_2O_2, H_2O_2 kinetics, H_2O_2 consumption (b) with the optimized conditions for every oxidant agent in real water spiked with As(III) (0.1 mg/L).

NaOCl showed significantly higher oxidative capacity than the process with H_2O_2 with As(III) oxidation of about 99.6% in 10 min (final concentration of 0.3 μg/L) (Fig. 3a). When NaOCl process was assisted by UVC radiation, the efficiency was comparable (99.8% with a final As concentration of 0.2 μg/L) to chlorine, but the treatment time was drastically reduced from 10 to 2 min. Both processes followed a zero-order kinetic, and the rate constant (k value) increased fivefold, from 9.7 to 49.9 M s^{-1} for NaOCl and UVC/NaOCl, respectively. This remarkable increase in the rate constant is attributed to the formation of radical species (Eqs. (4)–(10)) following the coupling UVC to NaOCl. The ability of UVC to accelerate the decomposition process allows for a higher reaction rate, even when the reaction follows zero-order kinetics,

Table 3
Optimal conditions for each process.

Process	Optimal oxidant concentration (mg/L)	As(III) oxidation efficiency (%)	Treatment Time (min.)
NaOCl	10.1	99.65	10
UVC/ NaOCl	5.1	99.81	2
H_2O_2	30.0	65.16	60
UVC/ H_2O_2	19.0	99.12	2

Table 4
Kinetic order and constants for each optimized process.

Process	Kinetic order	R^2	k
NaOCl	Zero	0.96	9.7 M s^{-1}
UVC/NaOCl	Zero	0.99	49.9 M s^{-1}
H_2O_2	Second	0.96	0.0004 M^{-1} s^{-1}
UVC/H_2O_2	Zero	0.96	49.8 M s^{-1}

emphasizing the crucial role of UVC as a potent powerful activating agent in this chemical system. Noteworthy, the oxidant concentration required to achieve the highest possible oxidation efficiency (according to RSM) decreases of about one half when the process was assisted by UVC radiation. When the H_2O_2 process was supported by UVC radiation, the oxidation of As(III) increased dramatically from 65.2% (final concentration of 34.84 μg/L) after 1 h to 99.1% after 2 min (final concentration of 0.9 μg/L). This behaviour is also supported by the fast oxidant consumption in the first few seconds until complete oxidation in 2 min (Fig. 3b). H_2O_2 and UVC/H_2O_2 processes followed a second-order kinetics in the dark and zero-order kinetics with the addition of UVC, with k values shifting from 4×10^{-4} M^{-1} s^{-1} for the H_2O_2 process to 49.8 M s^{-1} for the UVC/H_2O_2 process (Table 4). The transition from second-order kinetics in the dark to zero-order kinetics with the addition of UVC can be attributed to the role of UVC in accelerating the decomposition of H_2O_2. When the oxidation process occurs in the dark, it relies on the concentration of H_2O_2 as a limiting factor for the rate of the reaction. However, even in this case, coupling the UVC radiation to the oxidant, an efficient decomposition of H_2O_2 was promoted, making the reaction rate largely independent of the initial H_2O_2 concentration. This demonstrates the significant impact of UVC in altering the reaction pathway and kinetic behaviour, highlighting the shift from second-order to zero-order kinetics. While the oxidation of As(III) to As(V) with conventional oxidants has been quite exhaustively investigated in the past, that with HP-AOPs has received less attention, except for the UVC/H_2O_2 process. In a recent work, the only one to author knowledge where the RSM was applied to optimize the oxidant concentration for As(III) oxidation (Amiri et al., 2022), NaOCl was found to be the best oxidant compared to H_2O_2, and a concentration of about 9 mg/L lead to a 99.5% oxidation efficiency of As(III) in real water in 4 min (initial concentration of 200 μg/L), in agreement with our work. In particular, in their work with a double As(III) concentration, a double dose of NaOCl and a double treatment time were required to reach a similar As(III) oxidation efficiency. Taking into account the residual oxidant/disinfectant in drinking water is typically regulated, it is noteworthy that for the processes with NaOCl, UVC/NaOCl and UVC/H_2O_2, the final concentration of the oxidant is roughly 0.1 mg/L. This value guarantees a residual oxidant in the drinking water network and it is consistent with the recommended value of 0.2 mg/L set in the Legislative Decree 18/2023, following the adoption of European Directive EU 2020/2184 (European Parliament and Council, 2020). Whereas, in the process with H_2O_2 only, the oxidant residual concentration is roughly 4 mg/L, which is not consistent with the Italian regulation.

3.5. Adsorption of As(V)

Table 5 shows the comparison among the different adsorbing materials in the removal of As(V) from aqueous solution (initial As(V) concentration of 100 μg/L). Experiments were carried out using 50 and 100 mL of aqueous solution and 0.02 g of adsorbent. The amount of adsorbent (0.02 g) represents the lower quantity able to quantitatively remove As(V) under the investigated reaction conditions. Moreover, it allows to highlight differences, in terms of As(V) removal, between the investigated adsorbents. MgAl–Cl and ZnAl–NO_3 layered double hydroxides were found to be the most effectives in the removal of As(V) (92–98% after 1 min treatment). These adsorbents were tested in additional experiments for the treatment of 200 mL of As(V) contaminated aqueous solution. ZnAl–NO_3 layered double hydroxide showed outstanding results for As(V) removal in 200 mL of contaminated aqueous solution (93% after 1 min treatment). MgAl– NO_3 and ZnAl–Cl showed excellent results (96 and 92%, respectively, 1 min treatment) but As(V) removal efficiencies decreased when 100 mL of solution was used (68 and 56, respectively, 1 min treatment). Bayoxide E33 and γ-Al_2O_3 resulted in a lower adsorbent capacity (9% and 39%, 1 min treatment) under the investigated conditions, which can be attributed to the low contact time in the case of Bayoxide E33 in comparison with that generally requested for iron-based adsorbents (Gupta et al., 2021; Tang et al., 2011). γ-Al_2O_3 showed moderate adsorption ability toward As(V) and the obtained removals are lower than those reported in literature (90% after 10 min treatment, 0.2 g of γ-Al_2O_3, V = 100 mL) from drinking water (initial concentration of As(V) = 5 mg/L) (Iervolino et al., 2016). Mixed MgAl-oxide showed moderate capability as As(V) adsorbent and this result clearly highlight the crucial role of the layered double hydroxide structure to remove by anion exchange the arsenate from the water matrix. As a matter of fact, the higher adsorbent capability of the investigated LDHs was due to the properties/structures of these materials. LDHs exhibit, unlike of Bayoxide E33, γ-Al_2O_3 and mixed oxides, a peculiar structure, positively charged, balanced by interlayer anions (nitrate and chloride in this work), able to remove arsenate anions from water by anion exchange mechanism (Fierro et al., 2023). Arsenate was removed by their inclusion within the LDHs structure. The obtained results broaden the applicability of LHDs for real water treatments characterized by As(V) concentrations lower than 100 μg/L. Previous studies also reported interesting results in terms of As(V) removal in the presence of 50 mg/L As(V) solution using 0.2 g of calcined MgAl-LDH as adsorbent in 60–120 min treatment (Fierro et al., 2023; Lee et al., 2018).

Finally, tests were performed on drinking water ([As(V)] = 100 μg/L) to study the effect of interfering ions on MgAl–Cl and ZnAl–NO_3 layered double hydroxides adsorption efficiencies. Anions present in the water sample (sulphate, phosphate, nitrate, chloride, fluoride, etc.) can compete with the arsenate anion for the interlayer space of the investigated LDHs. As shown in Table 6, ZnAl–NO_3 showed the best results with high removal of As(V) (88%, 1 min) resulting in a final residual concentration of As(V) of 12 μg/L. Instead, adsorption capacity of MgAl–Cl reaches 57% after 5 min. Generally, the efficiencies observed in deionized water solutions change drastically when the same process is investigated in real water. These results clearly highlighted the limited effect of the interfering anions on ZnAl–NO_3 performances in contaminated drinking water for As(V) removal.

Table 5
Comparison among different adsorbing materials for As(V) (initial concentration 100 μg/L) removal in distilled water.

Adsorbent	As(V) removal (%)					
	V = 50 mL		V = 100 mL		V = 200 mL	
	t = 1 min	t = 5min	t = 1 min	t = 5min	t = 1min	t = 5min
MgAl–Cl	95 ± 2	95 ± 2	86 ± 1	92 ± 2	88 ± 1	78 ± 1
MgAl–NO_3	96 ± 2	96 ± 2	68 ± 1	83 ± 1	–	–
ZnAl–Cl	92 ± 2	96 ± 2	56 ± 1	99 ± 2	–	–
ZnAl– NO_3	96 ± 2	95 ± 2	98 ± 2	96 ± 2	93 ± 2	95 ± 2
γ-Al2O3	39 ± 1	59 ± 1	11 ± 1	57 ± 1	–	–
MgAl-mixed oxides	72 ± 1	45 ± 1	39 ± 1	49 ± 1	–	–
Bayoxide E33	9 ± 1	21 ± 2	0	0	–	–

4. Conclusion

The HP-AOPs were found to be more effective in the oxidation of As (III) to As(V) than the respective NaOCl and H_2O_2 oxidation processes in dark. The operating conditions were optimized by RSM tool, identifying 5.1 mg NaOCl/L and 19.0 mg H_2O_2/L as optimum oxidant doses for

Table 6
Comparison among MgAl–Cl and ZnAl– NO_3 for As(V) (initial concentration 100 μg/L) removal in drinking water (V = 100 mL).

Adsorbent	As(V) removal (%)			
	1 min	5 min	15 min	30 min
MgAl–Cl	52 ± 1	57 ± 2	44 ± 2	47 ± 2
ZnAl– NO_3	87 ± 2	87 ± 2	88 ± 2	87 ± 2

UVC/NaOCl and UVC/H_2O_2 processes, respectively, to be used in the subsequent kinetic tests.

The kinetic tests in real drinking water suggest that UVC/NaOCl is the most suitable process for the oxidation of As(III) to As(V). As matter of fact, while oxidation rate is comparable among UVC/NaOCl (99.8%), NaOCl (99.6%) and UVC/H_2O_2 (99.1%), a significantly shorter contact time (2 min) is necessary compared to NaOCl (10 min) and a lower oxidant dose (5.1 mg/L) compared to UVC/H_2O_2 (19.0 mg/L). Finally, As(V) produced by the photooxidation reaction of As(III) promoted by UVC/NaOCl can be effectively removed from drinking water through adsorption treatment with ZnAl–NO_3 (88% removal after 1 min treatment).

CRediT authorship contribution statement

Anna Melnikova: Investigation, Writing – original draft. **Antonio Faggiano:** Investigation, Methodology, Writing – original draft, Formal analysis. **Marco Visconti:** Investigation. **Raffaele Cucciniello:** Conceptualization, Writing – review & editing, Supervision, Resources. **Patrizia Iannece:** Formal analysis. **Natalia Kostryukova:** Supervision. **Antonio Proto:** Conceptualization, Methodology, Resources. **Antonino Fiorentino:** Conceptualization, Supervision, Writing – review & editing, Project administration, Validation. **Luigi Rizzo:** Conceptualization, Methodology, Supervision, Writing – review & editing, Funding acquisition.

Declaration of competing interest

The authors declare that they have no known competing financial interests or personal relationships that could have appeared to influence the work reported in this paper.

Data availability

Data will be made available on request.

Acknowledgements

AM and NK would like to thank the Ministry of Education and Science of the Russian Federation for the grant to support EA's internship at University of Salerno.

Appendix A. Supplementary data

Supplementary data to this article can be found online at https://doi.org/10.1016/j.jenvman.2023.119568.

References

Abenza, M., Rodríguez, J., de Labastida, M.F., de Pablo, J., Cortina, J.L., Martí, V., Vázquez-Suñé, E., Gibert, O., 2023. Reclamation of urban pollution impacted groundwater by advanced treatment processes: effect of prechlorination on the removal of metals, ammonium and NOM at pilot scale. J. Water Process Eng. 54, 103973 https://doi.org/10.1016/j.jwpe.2023.103973.

Alam, M.A., Mukherjee, A., Bhattacharya, P., Bundschuh, J., 2023. An appraisal of the principal concerns and controlling factors for Arsenic contamination in Chile. Sci. Rep. 13, 11168 https://doi.org/10.1038/s41598-023-38437-7.

Amiri, S., Vatanpour, V., He, T., 2022. Optimization of effective parameters in arsenite oxidation process with Cl2, H2O2, and O3 using response surface methodology. Chem. Eng. Process - Process Intensif. 181, 109167 https://doi.org/10.1016/j.cep.2022.109167.

Bundschuh, J., Armienta, M.A., Morales-Simfors, N., Alam, M.A., López, D.L., Delgado Quezada, V., Dietrich, S., Schneider, J., Tapia, J., Sracek, O., Castillo, E., Marco Parra, L.-M., Altamirano Espinoza, M., Guimarães Guilherme, L.R., Sosa, N.N., Niazi, N.K., Tomaszewska, B., Lizama Allende, K., Bieger, K., Alonso, D.L., Brandão, P.F.B., Bhattacharya, P., Litter, M.I., Ahmad, A., 2021. Arsenic in Latin America: new findings on source, mobilization and mobility in human environments in 20 countries based on decadal research 2010-2020. Crit. Rev. Environ. Sci. Technol. 51, 1727–1865. https://doi.org/10.1080/10643389.2020.1770527.

Chianese, L., Murcia, J.J., Hidalgo, M.C., Vaiano, V., Iervolino, G., 2023. Bismuth ferrite as innovative and efficient photocatalyst for the oxidation of As(III) to As(V) under visible light. Mater. Sci. Semicond. Process. 167, 107801 https://doi.org/10.1016/j.mssp.2023.107801.

Dodd, M.C., Vu, N.D., Ammann, A., Le, V.C., Kissner, R., Pham, H.V., Cao, T.H., Berg, M., Von Gunten, U., 2006. Kinetics and mechanistic aspects of As(III) oxidation by aqueous chlorine, chloramines, and ozone: relevance to drinking water treatment. Environ. Sci. Technol. 40, 3285–3292. https://doi.org/10.1021/es0524999.

European Parliament Council, 2020. Directive (EU) 2020/2184 of the European Parliament and of the Council of 16 December 2020 on the Quality of Water Intended for Human Consumption (Recast) (Text with EEA Relevance), vol. 2020.

Faggiano, A., Ricciardi, M., Motta, O., Fiorentino, A., Proto, A., 2023. Greywater treatment for reuse: effect of combined foam fractionation and persulfate-iron based fenton process in the bacterial removal and degradation of organic matter and surfactants. J. Clean. Prod. 415, 137792 https://doi.org/10.1016/j.jclepro.2023.137792.

Fierro, F., Lamparelli, D.H., Genga, A., Cucciniello, R., Capacchione, C., 2023. I-LDH as a heterogeneous bifunctional catalyst for the conversion of CO2 into cyclic organic carbonates. Mol. Catal. 538, 112994 https://doi.org/10.1016/j.mcat.2023.112994.

Fiorentino, A., Ferro, G., Alferez, M.C., Polo-López, M.I., Fernández-Ibañez, P., Rizzo, L., 2015. Inactivation and regrowth of multidrug resistant bacteria in urban wastewater after disinfection by solar-driven and chlorination processes. J. Photochem. Photobiol. B Biol. 148, 43–50. https://doi.org/10.1016/j.jphotobiol.2015.03.029.

Fiorentino, A., Rizzo, L., Guilloteau, H., Bellanger, X., Merlin, C., 2017. Comparing TiO2 photocatalysis and UV-C radiation for inactivation and mutant formation of Salmonella typhimurium TA102. Environ. Sci. Pollut. Res. Int. 24, 1871–1879. https://doi.org/10.1007/s11356-016-7981-6.

Ghezzi, L., Arrighi, S., Petrini, R., Bini, M., Vittori Antisari, L., Franceschini, F., Franchi, M.L., Giannecchini, R., 2023. Arsenic contamination in groundwater, soil and the food-chain: risk management in a densely populated area (Versilia plain, Italy). Appl. Sci. 13, 5446. https://doi.org/10.3390/app13095446.

Goswami, R., Kumar, M., Biyani, N., Shea, P.J., 2020. Arsenic exposure and perception of health risk due to groundwater contamination in Majuli (river island), Assam, India. Environ. Geochem. Health 42, 443–460. https://doi.org/10.1007/s10653-019-00373-9.

Gupta, A.D., Rene, E.R., Giri, B.S., Pandey, A., Singh, H., 2021. Adsorptive and photocatalytic properties of metal oxides towards arsenic remediation from water: a review. J. Environ. Chem. Eng. 9, 106376 https://doi.org/10.1016/j.jece.2021.106376.

Hao, L., Liu, M., Wang, N., Li, G., 2018. A critical review on arsenic removal from water using iron-based adsorbents. RSC Adv. 8, 39545–39560. https://doi.org/10.1039/C8RA08512A.

Iervolino, G., Vaiano, V., Rizzo, L., Sarno, G., Farina, A., Sannino, D., 2016. Removal of arsenic from drinking water by photo-catalytic oxidation on MoOx/TiO2 and adsorption on γ-Al2O3. J. Chem. Technol. Biotechnol. 91, 88–95. https://doi.org/10.1002/jctb.4581.

Iervolino, G., Zammit, I., Vaiano, V., Rizzo, L., 2019. Limitations and prospects for wastewater treatment by UV and visible-light-active heterogeneous photocatalysis: a critical review. Top. Curr. Chem. 378, 7. https://doi.org/10.1007/s41061-019-0272-1.

Jadhav, S.V., Häyrynen, P., Marathe, K.V., Rathod, V.K., Keiski, R.L., Yadav, G.D., 2018. Experimental and modeling assessment of sulfate and arsenic removal from mining wastewater by nanofiltration. Int. J. Chem. React. Eng. 16 https://doi.org/10.1515/ijcre-2016-0103.

Lee, G., Song, K., Bae, J., 2011. Permanganate oxidation of arsenic(III): reaction stoichiometry and the characterization of solid product. Geochem. Cosmochim. Acta 75, 4713–4727. https://doi.org/10.1016/j.gca.2011.02.043.

Lee, S.-H., Tanaka, M., Takahashi, Y., Kim, K.-W., 2018. Enhanced adsorption of arsenate and antimonate by calcined Mg/Al layered double hydroxide: investigation of comparative adsorption mechanism by surface characterization. Chemosphere 211, 903–911. https://doi.org/10.1016/j.chemosphere.2018.07.153.

Lescano, M., Zalazar, C., Cassano, A., Brandi, R., 2012. Kinetic modeling of arsenic (III) oxidation in water employing the UV/H2O2 process. Chem. Eng. J. 211 (212), 360–368. https://doi.org/10.1016/j.cej.2012.09.075.

Liu, L., Zhang, M., Suib, S.L., Qiu, G., 2022. Rapid photooxidation and removal of As(III) from drinking water using Fe-Mn composite oxide. Water Res. 226, 119297 https://doi.org/10.1016/j.watres.2022.119297.

Liu, R., Qu, J., 2021. Review on heterogeneous oxidation and adsorption for arsenic removal from drinking water. J. Environ. Sci. Key Lab. Drink. Water 110, 178–188. https://doi.org/10.1016/j.jes.2021.04.008.

Masindi, V., Gitari, W.M., 2016. Removal of arsenic from wastewaters by cryptocrystalline magnesite: complimenting experimental results with modelling. J. Clean. Prod. 113, 318–324. https://doi.org/10.1016/j.jclepro.2015.11.043.

Rizzo, L., 2022. Addressing main challenges in the tertiary treatment of urban wastewater: are homogeneous photodriven AOPs the answer? Environ. Sci.: Water Res. Technol. https://doi.org/10.1039/D2EW00146B.

Shaji, E., Santosh, M., Sarath, K.V., Prakash, P., Deepchand, V., Divya, B.V., 2021. Arsenic contamination of groundwater: a global synopsis with focus on the Indian Peninsula. Geosci. Front. 12, 101079 https://doi.org/10.1016/j.gsf.2020.08.015.

Sikder, R., Zhang, T., Ye, T., 2023. Predicting THM Formation and Revealing its Contributors in Drinking Water Treatment Using Machine Learning. ACS EST Water. https://doi.org/10.1021/acsestwater.3c00020.

Singh Patel, K., Kant Pandey, P., Martín-Ramos, P., Corns, T., Varol, S., Bhattacharya, P., Zhu, Y., 2023. A review on arsenic in the environment: contamination, mobility, sources, and exposure. RSC Adv. 13, 8803–8821. https://doi.org/10.1039/D3RA00789H.

Sorlini, S., Collivignarelli, C., 2011. Arsenic in Water for Human Consumption : Technical Solutions for Arsenic Removal from Drinking Water.

Sorlini, S., Gialdini, F., 2010. Conventional oxidation treatments for the removal of arsenic with chlorine dioxide, hypochlorite, potassium permanganate and monochloramine. Water Res. Groundwater Arsenic: From Genesis Sustain. Remed. 44, 5653–5659. https://doi.org/10.1016/j.watres.2010.06.032.

Sorlini, S., Gialdini, F., Stefan, M., 2010. Arsenic oxidation by UV radiation combined with hydrogen peroxide. Water Sci. Technol. 61, 339–344. https://doi.org/10.2166/wst.2010.799.

Srivastav, A.L., Patel, N., Chaudhary, V.K., 2020. Disinfection by-products in drinking water: occurrence, toxicity and abatement. Environ. Pollut. 267, 115474 https://doi.org/10.1016/j.envpol.2020.115474.

Tang, W., Li, Q., Gao, S., Shang, J.K., 2011. Arsenic (III,V) removal from aqueous solution by ultrafine α-Fe2O3 nanoparticles synthesized from solvent thermal method. J. Hazard Mater. 192, 131–138. https://doi.org/10.1016/j.jhazmat.2011.04.111.

Vaiano, V., Iervolino, G., Rizzo, L., 2018. Cu-doped ZnO as efficient photocatalyst for the oxidation of arsenite to arsenate under visible light. Appl. Catal. B Environ. 238, 471–479. https://doi.org/10.1016/j.apcatb.2018.07.026.

Vaiano, V., Iervolino, G., Sannino, D., Rizzo, L., Sarno, G., Farina, A., 2014. Enhanced photocatalytic oxidation of arsenite to arsenate in water solutions by a new catalyst based on MoOx supported on TiO2. Appl. Catal., B: Environ. 160–161, 247–253. https://doi.org/10.1016/j.apcatb.2014.05.034.

Welna, M., Pohl, P., Szymczycha-Madeja, A., 2019. Non-chromatographic speciation of inorganic arsenic in rice by hydride generation inductively coupled plasma optical emission spectrometry. Food Anal. Methods 12, 581–594. https://doi.org/10.1007/s12161-018-1388-6.

World Health Organizaion, 2022. Guidelines for Drinking-Water Quality, fourth ed. (incorporating the first and second addenda).

Zaw, M., Emett, M.T., 2002. Arsenic removal from water using advanced oxidation processes. Toxicol. Lett. 133, 113–118. https://doi.org/10.1016/S0378-4274(02)00081-4.

Zhang, X., Fan, H., Yuan, J., Tian, J., Wang, Y., Lu, C., Han, H., Sun, W., 2022. The application and mechanism of iron sulfides in arsenic removal from water and wastewater: a critical review. J. Environ. Chem. Eng. 10, 108856 https://doi.org/10.1016/j.jece.2022.108856.